Streptomyces alleviate abiotic stress in plant by producing pteridic acids

Zhijie Yang[1], Emil Strøbech[1], Yijun Qiao[1], Naga Charan Konakall[2], Pernille Harris[3], Gundela Peschel[4], Miriam Agler-Rosenbaum[4], Tilmann Weber[5], Erik Andreasson[2], Ling Ding[1,*]

[1] Department of Biotechnology and Biomedicine, Technical University of Denmark, Søltofts Plads, Building 221, 2800 Kgs. Lyngby, Denmark.

[2] Department of Plant Protection Biology, Swedish University of Agricultural Sciences, Sundsvägen 14, SE-230 53, Alnarp, Sweden.

[3] Department of Chemistry, Technical University of Denmark, Søltofts Plads, Building 206, 2800 Kgs. Lyngby, Denmark.

[4] Leibniz Institute for Natural Product Research and Infection Biology - Hans Knöll Institute (HKI), Beutenbergstr. 11a, 07745 Jena, Germany.

[5] Novo Nordisk Foundation Center for Biosustainability, Technical University of Denmark, Kemitorvet, Building 220, 2800 Kgs. Lyngby, Denmark.

*Corresponding author: Ling Ding lidi@dtu.dk

Abstract

Soil microbiota can confer fitness advantages to plants and increase crop resilience to drought and other abiotic stressors. However, there is little evidence on the mechanisms correlating a microbial trait with plant abiotic stress tolerance. Here, we report that *Streptomyces* effectively alleviates the drought and salinity stress by producing spiroketal polyketide pteridic acid H (**1**) and its isomer F (**2**), both of which promote root growth in *Arabidopsis* at a concentration of 1.3 nM under abiotic stress. Pteridic acids induce stress response genes expression in salinity-stressed *Arabidopsis* seedlings. The bifunctional biosynthetic gene cluster of pteridic acids and antimicrobial elaiophylin is confirmed in vivo and mainly disseminated by vertical transmission which is geographically distributed in various environments. This discovery reveals a perspective for understanding plant-*Streptomyces* interactions and provides a promising approach for utilising beneficial *Streptomyces* and their secondary metabolites in agriculture to mitigate the detrimental effects of climate change.

Introduction

According to the Food and Agriculture Organization of the United Nations, climate change generates considerable uncertainty about future water availability in many regions. Increased water scarcity under climate change will present a major challenge for climate adaptation, while sea-level rise will affect the salinity of surface and groundwater in coastal areas. Stress caused by climate change has led to increased agricultural losses and threatened global food security.[1,2] Drought is considered the most damaging environmental stress, which directly affects the entire growth period of plant seeds from germination to final fruiting.[3] Drought stress can lead to increased plant osmotic regulators, the inhibition of photosynthesis, and the change of plant endogenous hormone content.[4-6] Drought stress also induces reactive oxygen species (ROS), such as superoxide radicals, hydrogen peroxide, and hydroxyl radicals, leading to oxidative stress.[7] At high concentrations, ROS can cause damage at various tissue levels, for example, triggering lipid peroxidation and membrane degradation in plants.[8,9] Crop loss due to soil salinisation is another increasing threat to agriculture worldwide, which is more severe in agricultural land in coastal and arid regions.[10] Irrigation with saline water, low precipitation, and high evapotranspiration are key factors of the rapid salinisation of agricultural land.[11] These abiotic stresses of drought and salinity have brought unprecedented challenges to the development of crop farming. Compared to the heavy use of chemical fertilisers, the use of plant growth-promoting bacteria to improve plant growth under drought and salinity environments is more sustainable and gaining more attention.[12,13]

Soil microbial communities are critical to plant health and their resistance to both biotic and abiotic stressors, such as pathogens, drought, salinity, and heavy metal pollution.[14] A few studies have demonstrated that many beneficial soil bacteria harbour plant growth-promoting activities, *e.g.* by helping plants with disease suppression,[15] nutrient acquisition,[16] phosphorus uptake[17] and nitrogen fixations.[18] Beneficial root microbiota also regulates biosynthetic pathways in the plant itself, leading to differential alterations in the plant metabolome in response to stresses.[19] *Streptomyces* are Gram-positive filamentous bacteria, widely distributed in soil and marine environments. While they have long been considered the richest source of bioactive secondary metabolites,[20] *Streptomyces* have recently drawn attention as a class of plant growth-promoting bacteria that help plants respond to adversity stress.[21] The growing evidence showed that *Streptomyces* can promote plant growth or tolerance to stressors in direct or indirect ways, by secreting plant growth regulator auxin (indole-3-acetic acid, IAA) and siderophores, inducing systemic resistance in plants, and regulating the rhizosphere microbiome via producing antibacterial compounds or signalling molecules.[22-24] Notably, the commercial product Actinovate® and Mycostop® are two *Streptomyces*-based formulations that

have been widely used to suppress a wide range of diseases in a variety of crop groups as a biological fungicide/bactericide for the long term. Recently, the enrichment of *Streptomyces* has also been shown to play a subsequent role in the drought/salt tolerance of plants.[25] Despite the widespread claims of efficacy of inoculation of plant growth-promoting *Streptomyces*, the molecular basis of the growth-promoting effects and the key role of secondary/specialised metabolites in this process are largely unknown.

Here, we report that *Streptomyces iranensis* HM 35 has profound beneficial effects on helping barley alleviate osmotic, drought and salinity stress. The active components were identified as a bioactive spiroketal polyketide pteridic acids H (**1**) and its isomer F (**2**) through large-scale fermentation and bioactivity-directed purification followed by NMR, MS, and X-ray crystallography. The abiotic stress mitigating effect of pteridic acids H and F have been confirmed on the model plant *Arabidopsis thaliana,* where it effectively reversed both drought and salinity stress as phytohormone-like small biomolecules at concentrations as low as 0.5 ng mL^{-1} (1.3 nM). Moreover, the Biosynthetic Gene Cluster (BGC) of pteridic acids (*pta*) was identified and analysed in silico and functionally confirmed by in vivo CRISPR-based genome editing. We have furthermore conducted a survey of 81 potential producers of pteridic acids, which are widely distributed around the world. Phylogenetic and comparative genomic analysis of *pta*-containing *Streptomyces* suggested that these strains have evolutionary convergence in disseminating *pta* BGC through main vertical transmission and occasional horizontal gene transfer. In summary, we reveal a strategy of *Streptomyces* to secret plant growth regulators that help plants cope with abiotic stresses, which is a promising alternative solution for plant development and crop yields under the current climate change-induced environmental stresses.

Results

Abiotic Stress-Mitigating Activities Exhibited by *S. iranensis*. The promotion of barley growth induced by *S. iranensis* was tested under multiple abiotic stresses including osmotic, salinity and drought. The osmotic stress experiment was simulated using soils supplemented with 20% (w/v) PEG-6000 by transiently reducing the water potential (Ψ_W) of the plant. We found that the *S. iranensis* played a significant role in alleviating osmotic stress in barley seedlings. The treated seedlings showed a significant increase in height, fresh weight, and dry weight compared to the control group without any extra treatment (Fig. 1a). The culture broth of *S. iranensis* also showed considerable activity for the growth of barley in alleviating salinity stress mediated by 100 mM NaCl (Fig. 1b), while *S. iranensis* was not significantly enriched in the soil around the roots of barley seedlings (Supplementary Fig. 1). Additionally, based on the analysis of barley seedling phenotypes, the treatment with *S.*

iranensis resulted in a significant improvement in plant growth recovery from drought stress (Fig. 1c). Surprisingly, *S. iranensis* promoted the growth of barley seedlings even in non-stress growth condition and thus indicate that *S. iranensis* may have potential for use in biocontrol (Supplementary Fig. 2).

Genomic and metabolomic profiles of *S. iranensis*. To reveal the potential bioactive components, we first annotated BGCs responsible for the biosynthesis of secondary metabolites in *S. iranensis* using antiSMASH 6.0.[26] Genome sequence analysis of *S. iranensis* revealed the presence of 50 putative secondary metabolites BGCs with a variety of biosynthetic categories (Supplementary Tab. 1). The clusters 4, 7, 8, 9, 24, 32, 36 and 41 were annotated to have greater than 85% similarity with BGCs responsible for the biosynthesis of coelichelin, azalomycin, nigericin, elaiophylin, desferrioxamin, ectoine, rapamycin and hygrocin, respectively. Their corresponding products were also detected and identified through High-resolution Liquid Chromatography-tandem Mass Spectrometry (HR-LC-MS/MS) as well as Global Natural Products Social (GNPS) molecular networking (Fig. 1d, Supplementary Fig. 3).[27] However, there are still a number of metabolites of *S. iranensis* are still unknown. Since none of the previously identified compounds have been associated with mitigating abiotic stress in plants, we were prompted to expand the fermentation process and identify the potential bioactive compounds.

Characterisation of the bioactive compound pteridic acid. To uncover the bioactive components, fermentation of *S. iranensis* was scaled up to 175 litres and the culture broth was subjected to separation through open-column chromatography on Amberchrom CG161Me resin, silica gel, and Sephadex LH-20. Bioactivity-guided fractionation led to the isolation of bioactive compound **1** (15.0 mg) together with another structurally related compound **2** (4.0 mg) (Fig. 1e).

The bioactive component compound **1** was isolated as a white solid. Its formula of $C_{21}H_{34}O_6$ was deduced by *m/z* 383.2439 $[M+H]^+$ (calculated for 383.2428, Δ 2.84 ppm). The ^{1}H NMR spectrum exhibited signals for four olefinic protons (δ 7.33, 6.26, 6.13, 5.90) corresponding to two conjugated double bonds, four oxygen-bearing methines (δ 3.85, 3.69, 3.59, 3.43), five methyls, and other aliphatic protons. The ^{13}C NMR spectrum indicated the presence of one carbonyl group (δ 168.7) and one oxygen-bearing quaternary carbon (δ 103.2, C-11). The COSY spectrum established two partial substructures, which could be connected via a spiral function by analysing HSQC and HMBC correlations (Supplementary Fig. 4-11). Compound **1** was crystallised in methanol solution, and the structure was determined via X-ray crystallography (Supplementary Fig. 12). Therefore, compound **1** was identified as a new *Streptomyces*-derived natural product named pteridic acid H.

Compound **2**, a white solid, is an isomer of **1** since MS deduced the same molecular formula of $C_{21}H_{34}O_6$. The ^{1}H NMR spectrum exhibited signals for four olefinic protons (δ 7.16, 6.25, 6.07, 5.97)

corresponding to two conjugated double bonds, four oxygen-bearing methines (δ 3.88, 3.66, 3.56, 3.32), five methyls, and other aliphatic protons. The ^{13}C NMR spectrum indicated the presence of one carbonyl group (δ 170.2) and one oxygen-bearing quaternary carbon (δ 103.2, C-11). HSQC and HMBC correlations confirmed a spiroketal skeleton. NOESY spectrum confirmed its relative configurations, where correlations between H-21 and H-13 and H-15, H-7 and H-12a, and H6, H-10, and Me-18 were observed. The key NOESY correlations between H-7 and H-12a revealed a different spiroketal structure than **1** (Supplementary Fig. 11, 13-20). This can be reflected by the relative up-field NMR data for C-12 (δ 33.8 vs δ 37.5 in **1**). Compound **2** was identified as pteridic acid F, previously isolated from *Streptomyces pseudoverticillus* YN17707 and a marine-derived *Streptomyces* sp. SCSGAA 0027.[28,29]

Abiotic stress mitigation of pteridic acids *in planta*. Initially, we tested the effects of different concentrations of pteridic acids H and F on *Arabidopsis* growth in the absence of abiotic stress. A concentration of 0.5 ng ml^{-1} of both pteridic acids H and F was found to significantly promote the growth of *Arabidopsis* seedlings (Supplementary Fig. 21). Under drought stress, pteridic acid H at a concentration of 0.5 ng mL^{-1} increased the root length and fresh weight of *Arabidopsis* seedlings by 54.5% and 89%, respectively, and its activity was significantly better than the IAA and ABA at the same molar concentration (Fig. 2a, 2c). The treatment of pteridic acid F also showed great activity in alleviating drought stress, and the root length and fresh weight were increased by 30.5% and 56.7%, respectively (Fig. 2c). Pteridic acids H and F also showed significant activity in alleviating NaCl-mediated salinity stress (Fig. 2b. 2d). Compared to the non-treated groups, the treatment of 0.5 ng mL^{-1} pteridic acids H and F increased root length of *Arabidopsis* seedlings by 74.0% and 61.8%, as well as fresh weight by 126.2% and 110.9%, respectively (Fig. 2d).

To gain insights into how plants respond to pteridic acids, we performed quantitative real-time PCR (qRT-PCR) analysis to measure the expression levels of stress response genes TONOPLAST INTRINSIC PROTEIN 2;3 (TIP2;3) and SALT OVERLY SENSITIVE 1 (SOS1) in *Arabidopsis* seedlings, induced by pteridic acids H and F under salinity stress. Compared to the control, the relative expression level of TIP2;3 was significantly increased following both 1-hour and 24-hour treatments, while the transcript levels of SOS1 was down-regulated at 1-hour while up- regulated at 24-hour (Fig. 2e). This result indicated that pteridic acids H and F regulated the TIP2;3 and SOS1 to activate stress-resistance responses in plants.

A previous study suggested that pteridic acids A and B might have a plant growth-promoting effect like IAA and could stimulate the formation of adventitious roots in kidney beans.[28] However, we observed that pteridic acids H and F displayed the different IAA-induced phenotypes. Pteridic acids

163 did not exhibit the function to significantly promote lateral root growth of *Arabidopsis* seedlings like
164 IAA (Fig. 2f, 2g).[30] We also found that pteridic acids were also not capable of promoting the formation
165 of adventitious roots in kidney beans, as shown in Supplementary Fig. S22. Except for drought and
166 salinity stress, we also tested the $CuSO_4$-mediated heavy metal stress alleviation activity of pteridic
167 acids in mung beans. The results showed that the 1 ng mL^{-1} pteridic acid H was effective as ABA in
168 helping mung beans to relieve heavy metal stress (Supplementary Fig. S23). In conclusion, pteridic
169 acids H and F are widely applicable potent plant growth regulators produced by *Streptomyces* to assist
170 plants in coping with different abiotic stress.

171 **Biosynthesis of pteridic acids.** The retro-biosynthesis analysis indicated that pteridic acids could
172 derive from a modular type I polyketide synthase. A putative *pta* BGC was identified in the whole
173 genome sequence of S. *iranensis*, which shows 87% antiSMASH similarity to the BGC of elaiophylin
174 (BGC0000053 in MiBiG database).[31] The *pta* BGC spans approximately 56 kb and encodes 20
175 individual biosynthetic genes responsible for the biosynthesis of core polyketide backbones, precursor,
176 glycosylated substituents, transporters and regulators (Supplementary Tab. 2). The five consecutive
177 Type I polyketide synthase (PKS) encoding genes within the *pta* BGC consist of one loading module
178 and seven extender modules, which are sequentially extended to form a linear polyketide chain by
179 ketosynthase (KS) domain, acyltransferase (AT) domain, acyl carrier protein (ACP), with additional
180 ketoreductase (KR), dehydratase (DH), and enoyl reductase (ER) domains. The substrate specificity
181 predictions for individual AT domains fit well with the structure of pteridic acids (Supplementary Tab.
182 3). The last "Asn" residue is absent in the conserved Lys-Ser-Tyr-Asn tetrad of the KR domain in
183 module 3 (PtaB), which is predicted to be inactive (Supplementary Fig. 24). This is consistent with the
184 nonreduced carbonyl group on the α-carbon in module 3. The first DH domain in module 1 is inactive
185 since it does not have a conserved active motif LxxHxxGxxxxP (Supplementary Fig. 25). Following
186 the thioesterase-mediated release of the polyketide chain, the 6,6-spiroketal core structure is likely
187 formed by spontaneous spiroketalisation of the carbonyl group on C11 and the two hydroxyl groups
188 on C17 and C25. Following a loss of H_2O, two differentially oriented spirocyclic rings were formed
189 to yield pteridic acids F and H (Fig. 3a). Remarkably, pteridic acid H showed molecular instability
190 under extreme conditions. In the water solution with high temperature (65°C) or acidity (pH = 3),
191 pteridic acid H is transformed into pteridic acid F (Supplementary Fig. 26). A similar spontaneous
192 transformation from (*S*) to (*R*) chirality at the centre of the spiroketal ring was also observed in 6,6-
193 spiroketal avermectin.[32]

194 **CRISPR base editing in *S. iranensis*.** To validate the *in silico* prediction of BGC, we utilized the
195 efficient base editing tool CRISPR-cBEST to further confirm *pta* BGC.[33] As a non-model
196 *Streptomyces* strain, *S. iranensis* is hard to genetically manipulate through intergeneric conjugation.[34]
197 Therefore, the conjugation process was systematically optimised in this study (Supplementary Fig. 27).
198 The core polyketide synthase *ptaA* was targeted and inactivated by converting a TGG (Trp) codon at
199 position 916 into the stop codon TAA using CRISPR base editing. The editing event was confirmed
200 by PCR amplification and Sanger sequencing of the editing site (Fig. 3c). As expected, the production
201 of both pteridic acids and elaiophylin was abolished in *S. iranensis*/Δ*ptaA* (Fig. 3c). Plant experiments
202 showed that the treatment of *S. iranensis*/Δ*ptaA* fermentation suspension led to the abolishment of the
203 abiotic stress mitigating effects (Fig. 1a, 1b, 1c). To further confirm *pta* gene cluster, a bacterial
204 artificial chromosome (BAC) library of *S. iranensis* was constructed. BAC-based cross-
205 complementation of the *ptaA* in *S. iranensis*/Δ*ptaA* restored the production of pteridic acids and
206 elaiophylin (Supplementary Fig. 28).

207 Interestingly, based on isotope-labelled precursor feeding and partial cosmid sequencing-based
208 bioinformatics prediction, this BGC has long been inferred to be responsible for the biosynthesis of
209 the antibacterial elaiophylin.[35,36] In 2015, Zhou et al. reported that thioesterase in the last module
210 catalyse the formation of symmetrical macrodiolide using two units of linear elaiophylin monomeric
211 seco acid (Fig. 3b).[37] To confirm whether the biosynthesis of pteridic acids is also thioesterase-
212 dependent, site-specific mutations of residues Met-Glu-Asp to Ile-Lys-Met were introduced into the
213 active sites of the TE domain *in vivo* (Supplementary Fig. S29).[38] The HR-LC-MS/MS analysis
214 showed that the mutant strain (M2089I+E2090K+D2091M) no longer produced pteridic acids and
215 elaiophylin (Fig. 3d). Hence, we provide additional evidence via in vivo inactivation and site-directed
216 mutagenesis. Co-production of the plant growth-regulating pteridic acids and the antimicrobial
217 elaiophylin through a shared BGC is intriguing and points to possible joint efforts in helping plants
218 cope with biotic and abiotic stress.

219 **Geographical distribution of pteridic acid producers.** We surveyed available gene cluster family
220 (GCF) data for all bacteria in the BiG-FAM database.[39] We found that *pta* BGC (GCF_02696) is
221 strictly restricted to the *Streptomyces* genus. In addition, a total of 55 BGCs with high similarity to the
222 *pta* BGC were detected by BiG-SCAPE,[40] among a total of 9,386 type I polyketides BGCs in 1,965
223 *Streptomyces* from the NCBI assembly database. Through literature supplementation and data
224 dereplication of other reported producers without sequence information, at least 81 *Streptomyces* are
225 known to produce pteridic acids/elaiophylin or have specific *pta* BGC up to date (Supplementary Tab.
226 4). Based on the known sampling information, the *pta*-containing *Streptomyces* display a variety of

227 geographic distribution and biological origins (Fig. 4). We selected two available *Streptomyces* strains
228 (*Streptomyces violaceusniger* Tu 4113 and *Streptomyces rapamycinicus* NRRL 5491) to test the
229 potential plant growth-promoting activity of these potential pteridic acid producers. The HR-LC-
230 MS/MS analysis of both culture broths revealed that they shared similar metabolite profiles, and both
231 produced pteridic acids H and F (Supplementary Fig. 30). Treatment with both culture broths on barley
232 seedlings also exhibited significant plant growth-promoting activities under osmotic, salinity and
233 drought stress (Fig. 4b, 4c and 4d). This evidence suggests that this class of *Streptomyces* and its
234 specific secondary metabolite pteridic acids have unique ecological significance involved in plant
235 abiotic stress resistance.

236 **Phylogeny and evolution of *pta* BGC.** To explore the evolutionary clues of pteridic acid producers,
237 16S rRNA genes were initially used to assess the relatedness of the collected 34 potential producers
238 of pteridic acids with other *Streptomyces* strains that do not contain *pta* BGC. (Fig. 5a; Supplementary
239 Fig. 31). The results revealed that, except for *Streptomyces albus* DSM 41398 and *Streptomyces* sp.
240 GMR22, and other *pta*-containing *Streptomyces* strains cluster together and are distinct with divergent
241 lineages. To further confirm this hypothesis, two high-resolution *Streptomyces* housekeeping genes,
242 tryptophan synthase subunit beta (*trpB*) and RNA polymerase subunit beta (*rpoB*) were employed to
243 analyse the phylogeny relationship among these strains.[41] Consequently, only *S. albus* DSM 41398
244 was classified in a distinct phylogenetic lineage among the *Streptomyces* strains containing *pta* BGC.
245 The strict congruence among the clades of the housekeeping genes indicated dominant vertical
246 transmission and potential horizontal gene transfer of the *pta* BGC in *Streptomyces*.

247 A total of 15 *pta*-containing *Streptomyces* with complete genome sequence information were
248 selected to conduct the comparative genomics investigation. The genetic diversity in these
249 *Streptomyces* strains was initially revealed using genome sequence similarity analysis. Except for *S.*
250 *albus* DSM 41398 and *Streptomyces* sp. NA02950, we observed a high degree of similarity in the
251 aligned region, as indicated by both the average nucleotide identity (ANI) and the alignment
252 percentage (AP) among these strains (Supplementary Fig. 32). Genome synteny analysis revealed that
253 partial genome rearrangements happened among strains even with high sequence similarities
254 (Supplementary Fig. 33). Notably, the *pta* BGC in *S. albus* DSM 41398 (*pta-alb*) is located at the end
255 of the chromosome, a high variable region in *Streptomyces*, suggesting its existence by accepting
256 heterologous biosynthetic gene fragments. The nucleotide sequence alignment of *pta* BGC results
257 showed that *pta-alb* is relatively complete, and the similarity of core genes is proportional to
258 evolutionary relatedness (Fig. 5b). The metabolite profile of *S. albus* DSM 41398 also confirmed the
259 integrity of the *pta-alb* by detecting the production of elaiophylin and pteridic acid H (Supplementary

260 Fig. 34). To further assess the biosynthesis diversity in remaining genetically related strains, we
261 performed a BGCs similarity analysis (Supplementary Fig. 35, 36). The connections between their
262 secondary metabolites, BGCs, revealed that these vertically inherited *Streptomyces* strains also harbour
263 striking similarities. Combining phylogenetic and comparative genomics analysis, we expect that *S.*
264 *albus* DSM 41398 is evolutionarily the most distinct member from other *pta*-containing *Streptomyces*
265 strains and obtained the *pta* BGC via horizontal gene transfer. However, most *pta*-containing
266 *Streptomyces* strains have vertically inherited *pta* and other gene clusters from their ancient ancestors
267 that may be ecologically important and rarely studied.

268 **Discussion**

269 Drought and salinisation of soil are increasing globally, driving a reduction in crop yields that threatens
270 food security. Plant growth-promoting bacteria is a class of beneficial microorganisms that positively
271 interact with the plant to confer environmental stresses.[42,43] Although some *Streptomyces* species have
272 been reported to have plant growth-promoting activity, the molecules mediating such positive effects
273 are poorly understood. Deciphering the molecular mechanism is key to understanding the complex
274 plant microbiota interaction. In this study, we present an example of *S. iranensis* secreting a family of
275 secondary metabolites, pteridic acids, to assist plants to cope with abiotic stresses like osmotic, salinity
276 and drought. Pteridic acids H and F were chemically isolated, structurally characterised and functional
277 validated as plant-beneficial molecules.

278 Plants respond to the harsh environment by changing their physiological processes for better
279 survival.[44] Salt and drought stress signal transduction consists of ionic and osmotic homeostasis
280 signaling pathways, detoxification (i.e., damage control and repair) response pathways, and pathways
281 for growth regulation.[45] Aquaporins are membrane channels that facilitate the uptake of soil water and
282 mediate the regulation of root hydraulic conductivity in response to a large variety of environmental
283 stresses. [46] TIPs represent one family of aquaporins, and they are involved in regulating water flow in
284 response to osmotic challenges like drought or salinity for a plant cell.[47] In our study, treatment of
285 pteridic acids H and F resulted in a 2.1-fold and 2-fold increase in TIP2;3 transcripts at 1-hour and a
286 2.1-fold and 2.9-fold increase at 24-hour, respectively (Fig. 2e). SOS1 is a plasma membrane Na^+/H^+
287 antiporter, which is important for plant to alleviate salinity stress.[48] In response to the ionic toxicity
288 triggered by salt stress, plants rely on the Salt Overly Sensitive (SOS) pathway to transport excessive
289 Na^+ from the cytoplasm to the apoplast, thus ensuring endogenous ionic homeostasis.[49] The
290 overexpression of SOS1 could significantly increase the salt tolerance of *Arabidopsis* plants.[50] We
291 noticed that the relative expression of SOS1 was significantly enhanced after the 24-hour treatment of
292 pteridic acids, which preliminary revealed the molecular basis that endows it with stress resistance.

293 However, the exact mode of action of pteridic acids remains to be further investigated by for example
294 genome-wide transcriptomics screening for pteridic acids insensitive mutant plants.
295 Horizontal gene transfer is an integral driver of BGC evolution, revealing the independent processes
296 of species phylogeny and BGCs distribution.[51] However, vertical inheritance also influences BGCs
297 evolutionary dynamics, evident from BGCs conservation among closely related strains.[52] We found
298 that the *pta* BGC in *Streptomyces* are widely dispersed geographically and mainly inherited through
299 vertical gene transmission. Some of these strains have also been described to have remarkable
300 biocontrol capabilities. For example, *Streptomyces* sp. AgN23 activates *Arabidopsis* defence responses
301 to fungal pathogen infection by secreting plant elicitors,[53] *Streptomyces rhizosphaericus* 0250 and
302 *Streptomyces* sp. 5-10 displayed significant biocontrol potential to fusarium wilt of bitter gourd.[54,55]
303 The family of *pta*-containing *Streptomyces* was also previously described as a specific phylogenetic
304 lineage with the highest BGC abundance and largest genome size across diverse *Streptomyces-type*
305 strains.[56] Although the biosynthetic diversity of these *Streptomyces* is likely due to horizontal transfer
306 events that occurred relatively recently in their evolutionary history instead of genetic diversification
307 through a vertical transfer of BGCs. The multiple Type I PKSs presenting among these strains are
308 highly conserved based on genetic similarity network analysis. There is currently some evidence
309 supporting potential complex cross-BGC regulation in this class of *Streptomyces* strains. Jiang et al.
310 demonstrated that a TetR family transcriptional regulator, GdmRIII, controls the biosynthesis of
311 geldanamycin and elaiophylin meanwhile, in *Streptomyces autolyticus* CGMCC 0516.[57] Recently, He
312 et al. found that the rapamycin BGC-situated LAL family regulator RapH co-ordinately regulated the
313 biosynthesis of both rapamycin and elaiophylin in *S. rapamycinicus* NRRL 5491.[58] Although these
314 reports correspond to cross-regulation between evolutionarily conserved BGCs, more details of these
315 communications need to be investigated.
316 In conclusion, pteridic acids are secondary metabolites produced by *Streptomyces* enhancing plant
317 resistance to abiotic stress. This is a useful illustration of the bacterial metabolite-mediated alteration
318 of plants in response to environmental stress. It will open avenues for utilising *Streptomyces* to rewild
319 plant microbiomes and improve plant abiotic stress resistance to tackle climate change.[59]

320 **Methods**

321 **Strains, plasmids, and cultivation.** All strains and plasmids used in this study were listed in
322 Supplementary Tab. 5. All *Streptomyces* strains were obtained from the German Collection of
323 Microorganisms and Cell Cultures GmbH (DSMZ, Germany). All *Escherichia coli* strains were grown
324 in liquid/solid LB medium (5.0 g L^{-1} yeast extract, 10.0 g L^{-1} peptone, 10.0 g L^{-1} NaCl) at 37°C. All
325 *Streptomyces* strains were grown on SFM medium (20.0 g L^{-1} mannitol, 20.0 g L^{-1} soya flour, 20.0 g

326 L^{-1} agar), and the SFM medium with the addition of 120 mM calcium chloride solution was used for
327 the step of conjugation at 28°C. The ISP2 medium (4.0 g L^{-1} yeast extract, 10.0 g L^{-1} malt extract, 4.0
328 g L^{-1} dextrose, and 1.0 L distilled water) was used for liquid fermentation of all *Streptomyces* strains
329 used in plant assay and metabolomics analysis. Appropriate antibiotics were supplemented with the
330 following working concentrations: apramycin (50 µg mL^{-1}), chloramphenicol (25 µg mL^{-1}), and
331 kanamycin (50 µg mL^{-1}). All chemicals utilized in this study were from Sigma-Aldrich, USA.

332 **Metabolomics analyses.** High performance liquid chromatography was carried out on the Agilent
333 Infinity 1290 UHPLC system (Agilent Technologies, USA). The 250 × 2.1 mm i.d., 2.7 µm, Poroshell
334 120 Phenyl Hexyl column (Agilent Technologies, USA) was used for separation. The 2-µL samples
335 were eluted at a flow rate of 0.35 mL min^{-1} using a linear gradient from 10% acetonitrile in Milli-Q
336 water buffered with 20 mM formic acid increasing to 100% in 15 min. Each starting condition was
337 held for 3 min before the next run. Mass spectrometry detection was performed on an Agilent 6545
338 QTOF MS equipped with Agilent Dual Jet Stream electrospray ion source (ESI) with a drying gas
339 temperature of 160°C, a gas flow of 13 L min^{-1}, sheath gas temperature of 300°C, and flow of 16 L
340 min^{-1}. The capillary voltage was set to 4000 V and the nozzle voltage to 500 V in positive mode. MS
341 spectra were recorded as centroid data at an m/z of 100-1700, and auto MS/HRMS fragmentation was
342 performed at three collision energies (10, 20, and 40 eV) on the three most intense precursor peaks per
343 program. Data were analysed with MassHunter software (Agilent Technologies, USA) and compared
344 with known compounds and crude extract spectral libraries stored in the GNPS platform.[45] The
345 precursor and fragment ion mass tolerance were set as 0.1 Da and 0.02 Da, respectively. In addition,
346 the minpairs cos was set as 0.65, and the minimum matched fragment ions were set as 6.0. The
347 metabolites profile of wild-type *S. iranensis* was visualised by MS-Dial 4.9.2.[60]

348 **Large-scale fermentation and isolation.** *S. iranensis* was cultivated in medium 2 (3.0 g L^{-1}
349 $CaCl_2 \cdot 2H_2O$, 1.0 g L^{-1} citric acid/Fe III, 0.2 g L^{-1} $MnSO_4 \cdot H_2O$, 0.1 g L^{-1} $ZnCl_2$, 0.025 g L^{-1}
350 $CuSO_4 \cdot 5H_2O$, 0.02 g L^{-1} $Na_2B_4O_2 \cdot 10H_2O$, 0.01 g L^{-1} $NaMoO_4 \cdot 2H_2O$, and 20.0 g L^{-1} oatmeal in 1.0 L
351 distilled water), at 175 L filling volume in a 300 L fermentation vessel (Sartorius, Germany). The
352 fermentation was carried out for 6 days with aeration of 25-50 L min^{-1}, stirring at 200 rpm with a
353 temperature of 28°C and at a pH range of 5.4-6.4. The fermentation broth was separated, filtered, and
354 loaded onto an Amberchrom CG161Me resin LC column (200 × 20 cm, 6 L). Elution with a linear
355 gradient of H_2O-MeOH (from 30% to 100% v/v, flow rate 0.5 L min^{-1}, in 58 min) afforded seven
356 fractions (A-G). Fraction G was firstly fractionated by silica gel chromatography with a
357 CH_2Cl_2/CH_3OH gradient to yield 16 fractions, F01-F16. F07 was separated by a Sephadex LH-20

358 (MeOH) column and twelve sub-fractions F07a-l were obtained. From F07e, **1** (15.0 mg) and **2** (4.0
359 mg) were obtained by repeated HPLC RP-C_{18} (CH_3CN/H_2O as gradient).

360 Pteridic acid H (**1**): white solid; $[\alpha]_D^{20}$ 81 (0.32 mg/mL, CH_3OH), ^{1}H NMR (800 MHz, MeOD):
361 7.33 (dd, 15.4 Hz, 11.1 Hz, 1H), 6.26 (dd, 15.2 Hz, 10.8 Hz, 1H), 6.13 (dd, 15.3 Hz, 8.8 Hz, 1H), 5.90
362 (d, 15.4 Hz, 1H), 3.85 (dd, 10.2 Hz, 2.2 Hz, 1H), 3.69 (dd, 11.4 Hz, 4.9 Hz, 1H), 3.59 (m, 1H), 3.43
363 (m, 1H), 2.48 (m, 1H), 2.29 (dd, 14.9 Hz, 6.1 Hz, 1H), 2.01 (m, 1H), 1.64 (dd, 14.9 Hz, 1.9 Hz, 1H),
364 1.52 (m, 1H), 1.49 (m), 1.21 (d, 6.1 Hz, 3H), 1.01 (d, 6.8 Hz, 3H), 0.96 (d, 6.8 Hz, 3H), 0.93 (t, 7.3
365 Hz, 3H), 0.91 (d, 7.0 Hz, 3H); ^{13}CNMR (200 MHz, MeOD): 168.7, 151.0, 146.7, 129.6, 120.6, 103.2,
366 75.5, 72.8, 72.7, 70.3, 51.3, 42.2, 40.4, 37.5, 37.4, 24.8, 20.9, 16.0, 12.1, 11.1, 5.0; UV/vis
367 (CH_3CN/H_2O) λ_{max} 262 nm; IR (ATR) ν_{max} 2967, 2934, 2879, 1712, 1642, 1600, 1458, 1410, 1383,
368 1300, 1266, 1223, 1187, 1142, 1109, 1058, 1002, 973 cm^{-1}; (+)-HR-ESI-MS (*m/z*) $[M+H]^+$ calcd for
369 $C_{21}H_{35}O_6$, 383.2428; found, 383.2439. ^{1}H NMR and ^{13}C NMR see Supplementary Tab. 6.

370 Pteridic acid F (**2**): white solid; $[\alpha]_D^{20}$ -18 (10 mg/mL, CH_3OH), ^{1}H NMR (800 MHz, MeOD): 7.16
371 (dd, 15.1 Hz, 10.9 Hz, 1H), 6.25 (dd, 15.1 Hz, 10.9 Hz, 1H), 6.07 (dd, 15.1 Hz, 8.6 Hz, 1H), 5.97 (d,
372 15.1 Hz, 1H), 3.88 (m, 1H), 3.66 (td, 10.8 Hz, 4.3 Hz, 1H), 3.56 (dd, 11.5 Hz, 4.7 Hz, 1H), 3.32 (m,
373 1H), 2.49 (m, 1H), 2.19 (dd, 13.1 Hz, 4.3 Hz, 1H), 2.02 (m, 1H), 1.69 (m, 1H), 1.60 (m, 1H), 1.44 (m,
374 1H), 1.32 (dd, 13.2 Hz, 11.2 Hz, 1H), 1.14 (d, 6.2 Hz, 3H), 1.02 (m, 1H), 1.02 (d, 6.8 Hz, 3H), 0.95
375 (d, 6.9 Hz, 3H), 0.98 (d, 6.8 Hz, 3H), 1.60 (m, 1H), 1.44 (m, 1H), 0.82 (t, 7.6 Hz, 3H); ^{13}CNMR (200
376 MHz, MeOD): 170.2, 148.1, 143.4, 129,6, 122.9, 103.2, 77.7, 74.7, 69.8, 66.3, 52.2, 42.1, 40.5, 37.7,
377 33.8, 20.4, 19.7, 15.9, 12.7, 10.5, 5.3; UV/vis (CH_3CN/H_2O) λ_{max} 264 nm; IR (ATR) ν_{max} 2968, 2931,
378 2877, 1692, 1643, 1618, 1458, 1410, 1380, 1299, 1270, 1188, 1138, 1106, 1059, 1002, 973, 850 cm^{-1};
379 (+)-HR-ESI-MS (*m/z*): $[M+H]^+$ (calcd for $C_{21}H_{35}O_6$, 383.2428; found, 383.2433. ^{1}H NMR and ^{13}C
380 NMR see Supplementary Tab. 7.

381 **Structure identification.** NMR spectra were recorded on an 800 MHz Bruker Avance III spectrometer
382 equipped with a TCI CryoProbe using standard pulse sequences. NMR data were processed using
383 MestReNova 11.0. UHPLC-HRMS was performed on an Agilent Infinity 1290 UHPLC system
384 equipped with a diode array detector. UV-Vis spectra were recorded from 190 to 640 nm. Specific
385 rotations were acquired using Perkin-Elmer 241 polarimeter. IR data were acquired on Bruker Alpha
386 FTIR spectrometer using OPUS version 7.2. TLC analysis was performed on silica gel plates (Sil
387 G/UV_{254}, 0.20 mm, Macherey-Nagel). The Biotage Isolera One Flash Chromatography system was
388 used for flash chromatography and performed on silica gel 60 (Merck, 0.04–0.063 mm, 230–400 mesh
389 ASTM). Sephadex LH-20 was from Pharmacia.

390 **Crystal Structure Determination.** X-ray data collection of **1** was performed on an Agilent Supernova
391 Diffractometer using CuKα radiation. Data were processed and scaled using the CrysAlisPro software
392 (Agilent Technologies, USA). The structure was solved using SHELXS and refined using SHELXL.
393 Hydrogen atoms were included in ideal positions using riding coordinates. The absolute configuration
394 was determined based on the Flack parameter. Crystal Data for **1**: $C_{21}H_{34}O_6$, Mr = 382.50, monoclinic,
395 a = 8.4619(1) Å, b = 15.6161(2) Å, c = 8.4994(1) Å, α = 90.00°, β = 107.768(1)°, γ = 90.00°, V =
396 1069.55(2) Å3, T = 120(2) K, space group P21, Z = 2, μ(Cu Kα) = 0.698 mm–1, 17514 reflections
397 collected, 4275 independent reflections (Rint = 0.0226, Rsigma = 0.0155). The final R1 values were
398 0.0249 (I > 2σ(I)). The final wR2 values were 0.0648 (I > 2σ(I)). The final R1 values were 0.0252 (all
399 data). The final wR2 values were 0.0651 (all data). The goodness of fit on F2 was 1.057. The Flack
400 parameter is 0.13(10).

401 **Genetic manipulation.** All primers used were synthesised by IDT (Integrated DNA Technologies,
402 USA) and listed in Supplementary Tab. 8. Plasmids and genomic DNA purification, PCR and cloning
403 were conducted according to standard procedures using manufacturer protocols. PCR was performed
404 using OneTaq Quick-Load 2X Master Mix with Standard Buffer (New England Biolabs, USA). DNA
405 assembly was done by using NEBuilder HiFi DNA Assembly Master Mix (New England Biolabs,
406 USA). DNA digestion was performed with FastDigest restriction enzymes (Thermo Fisher Scientific,
407 USA). NucleoSpin Gel and PCR Clean-up Kits (Macherey-Nagel, Germany) were used for DNA
408 clean-up from PCR products and agarose gel extracts. One Shot Mach1 T1 Phage-Resistant
409 Chemically Competent *E. coli* (Thermo Fisher Scientific, USA) was used for cloning. NucleoSpin
410 Plasmid EasyPure Kit (Macherey-Nagel, Germany) was used for plasmid preparation. Sanger
411 sequencing was carried out using a Mix2Seq Kit (Eurofins Scientific, Luxembourg). All DNA
412 manipulation experiments were conducted according to standard procedures using manufacturer
413 protocols.

414 **Gene inactivation and site-directed mutagenesis.** To use the pCRISPR-cBEST for base editing
415 applications, an oligo was designed as Del-ptaA by the online tool CRISPy-web, and the pCRISPR-
416 cBEST plasmid was linearised by *Nco*I. Mixing the linearised pCRISPR-cBEST plasmid and Del-ptaA
417 with the NEBuilder HiFi DNA Assembly Master Mix (New England Biolabs, USA). The linearised
418 pCRISPR-cBEST plasmid was then bridged by Del-ptaA, ending with the desired pCRISPR-
419 cBEST/Δ*ptaA*. Chemically competent *E. coli* were transformed with the recombinant plasmid and
420 confirmed via PCR amplification (program: 94°C for 30 s, followed by 30 cycles consisting of 94°C
421 for 15 s; 54°C for 15 s; 68°C for 40 s, and 68°C for 2 min) and Sanger sequencing. The experimental

422 procedure for site-directed mutagenesis for the TE domain is the same as described above. The *E. coli-*
423 *Streptomyces* conjugation experiment was conducted according to the modified protocol in this study,
424 and the mutant *Streptomyces* strains were also confirmed by PCR and Sanger sequencing (Eurofins,
425 France).

426 **Construction of BAC and genetical complementation.** The BAC library of *S. iranensis* was
427 constructed using pESAC13-A from Bio S&T (Montreal, Canada). Based on a high-throughput
428 screening method (unpublished), we selected two BACs 1J23 and 6M10 that cross-cover the *ptaA* gene
429 (Supplementary Fig. 28). The selected BAC clones were further confirmed using four sets of primers,
430 including ID-1J23-right-F/R, ID-1J23-left-F/R, ID-6M10-right-F/R, and ID-6M10-left-F/R
431 (Supplementary Tab. 8). Subsequently, we introduced these two BAC clones 1J23 and 6M10 into *S.*
432 *iranensis*/Δ*ptaA* (remove the pCRISPR-cBEST/Δ*ptaA* to obtain antibiotics resistance free strain)
433 separately by conjugation. Exconjugants of mutants were further validated by apramycin-resistance
434 screening and PCR.

435 **Enrichment evaluation of *S. iranensis* in rhizosphere soil**. The *S. iranensis* (with the apramycin
436 resistance gene) spore suspension was well mixed with fully sterilised soil and was transferred to a
437 250 mL flask. The sterilised germinated barley seed was placed in the centre position of soil in flask
438 and grown at 24 ± 2°C, 8 h dark/16 h light in the growth chamber for 7 days. Samples were collected
439 from soil within 0.1 cm and 3 cm distance from the barley root, with a specification of 0.1 g soil per
440 sample. Then, these samples were transferred to sterilised 1.5 mL Eppendorf tubes and mixed with
441 500 μL sterilised H_2O. 200 μL of each sample was Spread evenly over the solid MS medium with the
442 addition of 50 μg mL^{-1} apramycin and grown at 28°C for 7 days. The number of *Streptomyces* colonies
443 grown on each plate were counted and statistically analysed.

444 ***Arabidopsis* growth assays.** *A. thaliana* ecotype Columbia (Col-0) was used to test the effects of
445 pteridic acid treatment under drought stress mediated by PEG-6000 (Duchefa Biochemie BV) and
446 salinity stress mediated by NaCl (Duchefa Biochemie BV). The modified Murashige & Skoog medium
447 (2.2 g L^{-1} Murashige & Skoog medium including B5 vitamins, 5.0 g L^{-1} of sucrose, 250 mg L^{-1} MES
448 monohydrate, 7.0 g L^{-1} agar, and adjusted pH to 5.7 with KOH) was used in this study. PEG-6000 (15%
449 w/v) was dissolved in water and filtered through 0.2-micron Sartorius Minisart™ Plus Syringe Filters
450 (Fisher Scientific). 50 mL of the filtered solution was overlaid onto the surface of solidified Murashige
451 & Skoog medium. The plates were left for 24 h to diffuse the PEG into the Murashige & Skoog medium.
452 NaCl was added to the medium to a final concentration of 80 mM for the salinity stress alleviation test.
453 The pure compound pteridic acids H and F (0.50 ng/mL), IAA (0.23 ng/mL), and ABA (0.34 ng/mL)

were mixed with different media to a final concentration of approximately 1.3 nM and poured into the plates. Seeds were surface sterilised by washing with 70% ethanol for 2 min, then in sterilisation solution (10% bleach) for 1 min by inverting the tubes, and finally washed five times with sterilised water. The seeds were stratified for 2 days at 4°C in the dark. Sterilised seeds were placed in Petri dishes (approx. 100 seeds per Petri dish) on Murashige & Skoog medium and grown for 3-4 days in the vertical position in a culture chamber at 22°C under standard long-day conditions (16/8 h light/dark photoperiod). After three days of growth, seedlings with similar root lengths (7-10 mm) were transferred to square plates containing Murashige & Skoog medium (control) or Murashige & Skoog medium supplemented with 15% (w/v) PEG-6000 or 80 mM NaCl. 16 seedlings were used per replicate for each treatment. The initial position of the plant root tip was marked with a marker. The plants were grown in the vertical position under standard long day conditions (22°C, 16/8h light/dark) for 8 days, and then each plate was scanned using Image Scanner. Primary and lateral root lengths and the total plant weight were then scored. The primary and lateral root length measurements were performed by analysing pictures with the Image J software. Fresh weight measurements were estimated using a precision balance. Whole 8-day-old plants grown in the medium were removed using forceps, dried in tissue paper, and then weighed using a precision balance.

Barley and mung bean growth assays. The pteridic acid *Streptomyces* producers were tested for their effects on barley cultivars Guld grown in soil. *S. iranensis* HM 35, *S. rapamycinicus* NRRL 5491, and *S. violaceusniger* Tu 4113 were cultivated in ISP2 medium for 7 days at 28˚C. 500 µL culture broth (ca. 3 x 10^9 CFU/mL) was added to 100 g sand soil and well mixed. Treated soils were infiltrated with Milli-Q water, 20% PEG-6000 solutions to simulate osmotic stress, and 100 mM NaCl solutions to simulate salinity stress in soil environments. To simulate drought stress during barley growth, the plant was initially watered for 7 days, then subjected to 7 days of drought stress, and finally allowed to recover with various treatments for another 7 days. Barley seeds were rinsed in distilled water and sterilised with 1% sodium hypochlorite for 15 min. They were then washed with distilled water and germinated in distilled water at 24°C for 2 days. Barley seeds were planted in each plastic pot (5cm x 5cm x 6cm, six seedlings per pot) supplemented with different treated soil and grown at 24 ± 2°C, 8 h dark/16 h light in the growth chamber for 7 days. Plant height (cm) was measured as the aerial part of the plant, and the fresh shoot weight (g) and fresh root weight (g) of each seedling were measured separately. Then, the seedlings were dried in the hot-air oven at 70°C for 6 h to obtain the dry shoot and dry root weights (g). For heavy metal stress experiment, mung beans were pre-germinated and placed on top of the modified Murashige & Skoog medium agar, supplemented with 10 mM CuSO4, with 1.0 ng/mL pure substances. All mung beans were grown in the dark at 24 ± 2°C for 4 days.

487 **Kidney beans growth assays**. The seeds of kidney beans (appr. 2 cm in length, from organic farming)
488 were firstly sterilised successively with ethanol (70% v/v) and sodium hypochlorite (5% v/v), each for
489 2 min and then rinsed with sterile Milli-Q water (three times). The sterilised seeds were cultivated on
490 modified Murashige & Skoog agar plates for 3-4 days. After germination, the seedlings (with 1.5-2
491 cm-long roots) were soaked in 10 mL aliquots of testing compounds (pteridic acids H and F, 1.0 ng/mL,
492 dissolved in sterile Milli-Q water) in ultra-clear polypropylene containers (ø 34 mm, vol. 20 mL) with
493 polyethylene caps. The control group was treated with 10 mL sterile Milli-Q water. For each treatment,
494 three repetitions (containers) were used, and each repetition included four seedlings. After 24 h, the
495 seeds were transferred into a cut square petri dish, put on the top layer of sandy soil, and then incubated
496 vertically in a growth chamber (24/22°C, day/night cycle of 16/8 h, 50%, 60%, 70%, 100% of
497 circulated wind velocity for 12 h, 2 h, 2h, 8h) for 7 days. Solutions of pteridic acids H and F (2 mL,
498 1.0 ng/mL for both) were added separately into corresponding containers, with sterile Milli-Q water
499 as control, and an extra 8 mL of Milli-Q water was added to each petri dish every other day.

500 **RNA extraction and quantitative real-time PCR**. *Arabidopsis* seeds were sterilized, and seven to
501 ten seeds were cultured in each well of a 24 well plate in 2 mL medium containing modified Murashige
502 & Skoog and 30 mM sucrose with 16 hours light, at 24 °C in a controlled environment room. After 7
503 days, seedlings were washed in 20 mL modified Murashige & Skoog medium and then moved to 20
504 mL of fresh medium and cultured in 125ml E-flasks with 1 ng mL^{-1} of each pteridic acids H and F.
505 Samples were collected at three Total RNA was extracted using RNeasy Plant Mini Kit (Qiagen,
506 Germany) according to the manufacturer's instructions. Reverse transcription was performed using
507 SuperScript™ III First-Strand Synthesis SuperMix for qRT-PCR (Invitrogen, USA). qRT-PCR was
508 conducted on CFX96 Touch Real-Time PCR Detection System (Bio-Rad, USA) using Platinum SYBR
509 Green qPCR SuperMix-UDG with ROX (Invitrogen, USA). The thermal cycling program consisted
510 of an initial denaturation at 95 ℃ for 3 min, followed by 39 cycles of 95 ℃ for 15 s, 60 ℃ for 30 s.
511 Three independent biological replicates were performed for each condition. TIP2;3 and SOS1 were
512 used as target genes, and primers sequences were given in Supplementary Tab. 8. The expression level
513 of target gene after treatments was calculated using the 2^ΔΔCt method, with ACT1 as the internal
514 control.

515 **Bioinformatics analyses**. The identification and annotation of all BGCs of *Streptomyces* secondary
516 metabolites were carried out with antiSMASH 6.0.[26] The threshold for similar BGCs was selected as
517 greater than 45% sequence similarity. The BiG-FAM database and BiG-SCAPE software were used
518 to identify the distribution of *pta* BGC in different bacteria and generate the *pta* family similarity

network.[39,40] A cut-off of 0.3 was used as a raw index similarity metric for the BiG-SCAPE analysis. The alignment of 15 *pta*-containing *Streptomyces* genome sequences was performed using the whole-genome alignment plugin of the CLC Genomics Workbench version 22.0.2 (Qiagen). The minimum initial seed length was 15 bp, and the minimum alignment block length was 100 bp. The networks of Big-SCAPE and GNPS analysis were visualised using Cytoscape 3.9. The phylogenetic analysis was conducted by the online multiple sequence alignment tool MAFFT and visualised by iTOL v5. [61,62]

Statistical analysis. Statistical significance was assessed by one-way ANOVA with post hoc Dunnett's multiple comparisons test, one-way ANOVA with Tukey test or t test (see each figure legends). All analyses were performed using GraphPad Prism version 9. P-values < 0.05 were considered significant. Asterisks indicate the level of statistical significance: $^{*}P < 0.05$, $^{**}P < 0.01$, $^{***}P < 0.001$, and $^{****}P < 0.0001$. For all relevant figures, source data and exact P values are provided in the Source Data file.

Data availability. The gene sequences used in this study were collected by searching National Center for Biotechnology Information (NCBI) or extracting from assembled genome sequences (attached in Supplementary information files). All genome sequences used in this study are publicly available on NCBI. The crystal structure was deposited at Cambridge Crystallographic Data Centre (https://www.ccdc.cam.ac.uk/) with CCDC deposition number 1984025. Metabolomics data in this study were deposited at https://massive.ucsd.edu with the identifier MSV000090745. Source data of each figure are provided with this paper.

References

1. Naylor, R., et al. A 20-year retrospective review of global aquaculture. *Nature* **591**, 551-563 (2021).
2. Wheeler, T. & von Braun, J. Climate change impacts on global food security. *Science* **341**, 508-513 (2013).
3. Zhang, H., Zhu, J., Gong, Z. & Zhu, J. Abiotic stress responses in plants. *Nat. Rev. Genet.* **23**, 104-119 (2022).
4. Kuromori, T., Fujita, M., Takahashi, F., Yamaguchi-Shinozaki, K. & Shinozaki, K. Inter-tissue and inter-organ signaling in drought stress response and phenotyping of drought tolerance. *Plant J.* **109**, 342-358 (2022).
5. Dos Santos, V., et al. Causes of reduced leaf-level photosynthesis during strong El Niño drought in a central Amazon forest. *Global Change Biol.* **24**, 4266-4279 (2018).
6. Waadt, R., et al. Plant hormone regulation of abiotic stress responses. *Nat. Rev. Mol. Cell Biol.* **23**, 680-694 (2022).

551 7. Kerchev, P. & Van Breusegem, F. Improving oxidative stress resilience in plants. *Plant J.* **109**, 359-
552 372 (2022).
553 8. Abid, M., et al. Physiological and biochemical changes during drought and recovery periods at
554 tillering and jointing stages in wheat (*Triticum aestivum* L.). *Sci. Rep.* **8**, 1-15 (2018).
555 9. Hasanuzzaman, M., et al. Regulation of ROS metabolism in plants under environmental stress: a
556 review of recent experimental evidence. *Int. J. Mol. Sci.* **21**, (2020).
557 10. Van Zelm, E., Zhang, Y. & Testerink, C. Salt tolerance mechanisms of plants. *Annu. Rev. Plant*
558 *Biol.* **71**, 403-433 (2020).
559 11. Corwin, D. Climate change impacts on soil salinity in agricultural areas. *Eur. J. Soil Sci.* **72**, 842-
560 862 (2021).
561 12. Hong, Y., Zhou, Q., Hao, Y. & Huang, A. C. Crafting the plant root metabolome for improved
562 microbe-assisted stress resilience. *New Phytol.* **234**, 1945-1950 (2022).
563 13. De Vries, F., Griffiths, R., Knight, C., Nicolitch, O. & Williams, A. Harnessing rhizosphere
564 microbiomes for drought-resilient crop production. *Science* **368**, 270-274 (2020).
565 14. Arif, I., Batool, M. & Schenk, P. Plant microbiome engineering: expected benefits for improved
566 crop growth and resilience. *Trends Biotechnol.* **38**, 1385-1396 (2020).
567 15. Berlanga-Clavero, M., et al. *Bacillus subtilis* biofilm matrix components target seed oil bodies to
568 promote growth and anti-fungal resistance in melon. *Nat. Microbiol.* **7**, 1-15 (2022).
569 16. Das, P., et al. Plant-soil-microbes: A tripartite interaction for nutrient acquisition and better plant
570 growth for sustainable agricultural practices. *Environ. Res.* **214**, 113821 (2022).
571 17. Hiruma, K., et al. Root endophyte *Colletotrichum tofieldiae* confers plant fitness benefits that are
572 phosphate status dependent. *Cell* **165**, 464-474 (2016).
573 18. Henneron, L., Kardol, P., Wardle, D., Cros, C. & Fontaine, S. Rhizosphere control of soil nitrogen
574 cycling: a key component of plant economic strategies. *New Phytol.* **228**, 1269-1282 (2020).
575 19. Etalo, D., Jeon, J. & Raaijmakers, J. Modulation of plant chemistry by beneficial root microbiota.
576 *Nat. Prod. Rep.* **35**, 398-409 (2018).
577 20. Quinn, G., Banat, A., Abdelhameed, A. & Banat, I. *Streptomyces* from traditional medicine: sources
578 of new innovations in antibiotic discovery. *J. Med. Microbiol.* **69**, 1040-1048 (2020).
579 21. Viaene, T., Langendries, S., Beirinckx, S., Maes, M. & Goormachtig, S. *Streptomyces* as a plant's
580 best friend? *FEMS Microbiol. Ecol.* **92**, (2016).
581 22. Myo, E., et al. Indole-3-acetic acid production by *Streptomyces fradiae* NKZ-259 and its
582 formulation to enhance plant growth. *BMC Microbiol.* **19**, 1-14 (2019).
583 23. Sadeghi, A., et al. Plant growth promoting activity of an auxin and siderophore producing isolate
584 of *Streptomyces* under saline soil conditions. *World J. Microbiol. Biotechnol.* **28**, 1503-1509 (2012).

585 24. Singh, S. & Gaur, R. Endophytic *Streptomyces* spp. underscore induction of defense regulatory
586 genes and confers resistance against *Sclerotium rolfsii* in chickpea. *Biol. Control* **104**, 44-56 (2017).
587 25. Fitzpatrick, C., et al. Assembly and ecological function of the root microbiome across angiosperm
588 plant species. *Proc. Natl. Acad. Sci. U. S. A.* **115**, E1157-E1165 (2018).
589 26. Blin, K., et al. antiSMASH 6.0: improving cluster detection and comparison capabilities. *Nucleic*
590 *Acids Res.* **49**, W29-W35 (2021).
591 27. Wang, M., et al. Sharing and community curation of mass spectrometry data with Global Natural
592 Products Social Molecular Networking. *Nat. Biotechnol.* **34**, 828-837 (2016).
593 28. Igarashi, Y., Iida, T., Yoshida, R. & Furumai, T. Pteridic acids A and B, novel plant growth
594 promoters with auxin-like activity from *Streptomyces hygroscopicus* TP-A0451. *J. Antibiot.* **55**, 764-
595 767 (2002).
596 29. Nong, X., Wei, X. & Qi, S. Pteridic acids C-G spirocyclic polyketides from the marine-derived
597 *Streptomyces* sp. SCSGAA 0027. *J. Antibiot.* **70**, 1047-1052 (2017).
598 30. Lavenus, J., et al. Lateral root development in *Arabidopsis*: fifty shades of auxin. *Trends Plant Sci.*
599 **18**, 455-463 (2013).
600 31. Kautsar, S., et al. MIBiG 2.0: a repository for biosynthetic gene clusters of known function. *Nucleic*
601 *Acids Res.* **48**, D454-D458 (2020).
602 32. Sun, P., et al. Spiroketal formation and modification in avermectin biosynthesis involves a dual
603 activity of AveC. *J. Am. Chem. Soc.* **135**, 1540-1548 (2013).
604 33. Tong, Y., et al. Highly efficient DSB-free base editing for streptomycetes with CRISPR-BEST.
605 *Proc. Natl. Acad. Sci. U. S. A.* **116**, 20366-20375 (2019).
606 34. Netzker, T., et al. An efficient method to generate gene deletion mutants of the rapamycin-
607 producing bacterium *Streptomyces iranensis* HM 35. *Appl. Environ. Microbiol.* **82**, 3481-3492 (2016).
608 35. Gerlitz, M., Hammann, P., Thiericke, R. & Rohr, J. The biogenetic origin of the carbon skeleton
609 and the oxygen atoms of elaiophylin, a symmetric macrodiolide antibiotic. *J. Org. Chem.* **57**, 4030-
610 4033 (1992).
611 36. Haydock, S., Mironenko, T., Ghoorahoo, H. & Leadlay, P. The putative elaiophylin biosynthetic
612 gene cluster in *Streptomyces* sp. DSM4137 is adjacent to genes encoding adenosylcobalamin-
613 dependent methylmalonyl CoA mutase and to genes for synthesis of cobalamin. *J. Biotechnol.* **113**,
614 55-68 (2004).
615 37. Zhou, Y., Prediger, P., Dias, L., Murphy, A. & Leadlay, P. Macrodiolide formation by the
616 thioesterase of a modular polyketide synthase. *Angew. Chem. Int. Ed.* **54**, 5232-5235 (2015).
617 38. Du, L. & Lou, L. PKS and NRPS release mechanisms. *Nat. Prod. Rep.* **27**, 255-278 (2009).
618 39. Kautsar, S., Blin, K., Shaw, S., Weber, T. & Medema, M. BiG-FAM: the biosynthetic gene cluster

619 families database. *Nucleic Acids Res.* **49**, D490-D497 (2021).
620 40. Navarro-Munoz, J., et al. A computational framework to explore large-scale biosynthetic diversity.
621 *Nat. Chem. Biol.* **16**, 60-68 (2020).
622 41. Komaki, H. Resolution of housekeeping gene sequences used in MLSA for the genus *Streptomyces*
623 and reclassification of *Streptomyces anthocyanicus* and *Streptomyces tricolor* as heterotypic synonyms
624 of *Streptomyces violaceoruber*. *Int. J. Syst. Evol. Microbiol.* **72**, 005370 (2022).
625 42. Coban, O., De Deyn, G. & van der Ploeg, M. Soil microbiota as game-changers in restoration of
626 degraded lands. *Science* **375**, eabe0725 (2022).
627 43. De Souza, R., Ambrosini, A. & Passaglia, L. M. P. Plant growth-promoting bacteria as inoculants
628 in agricultural soils. *Genet. Mol. Biol.* **38**, 401-419 (2015).
629 44. Lopes, M., Dias, M. & Gurgel, E. Successful plant growth-promoting microbes: inoculation
630 methods and abiotic factors. *Front. sustain. food syst.* **5**, 606454 (2021).
631 45. Zhu, J. Salt and drought stress signal transduction in plants. *Annu. Rev. Plant Biol.* **53**, 247-273
632 (2002).
633 46. Maurel, C., et al. Aquaporins in plants. *Physiol. Rev.* **95**, 1321-1358 (2015)
634 47. Kaldenhoff, R. & Fischer, M. Functional aquaporin diversity in plants. *Biochim. Biophys. Acta*
635 *Biomembr.* **1758**, 1134-1141 (2006).
636 48. Shi, H., Ishitani, M., Kim, C. & Zhu, J. The *Arabidopsis thaliana* salt tolerance gene SOS1 encodes
637 a putative Na^+/H^+ antiporter. *Proc. Natl. Acad. Sci. U. S. A.* **97**, 6896-6901 (2000).
638 49. Ji, H., et al. The Salt Overly Sensitive (SOS) pathway: established and emerging roles. *Mol. Plant*
639 **6**, 275-286 (2013).
640 50. Shi, H., Lee, B., Wu, S. & Zhu, J. Overexpression of a plasma membrane Na^+/H^+ antiporter gene
641 improves salt tolerance in *Arabidopsis thaliana*. *Nat. Biotechnol.* **21**, 81-85 (2003).
642 51. McDonald, B. & Currie, C. Lateral gene transfer dynamics in the ancient bacterial genus
643 *Streptomyces*. *Mbio* **8**, e00644-17 (2017).
644 52. Chase, A., Sweeney, D., Muskat, M., Guillen-Matus, D. & Jensen, P. Vertical inheritance facilitates
645 interspecies diversification in biosynthetic gene clusters and specialized metabolites. *Mbio* **12**, e02700-
646 21 (2021).
647 53. Vergnes, S., et al. Phyllosphere colonization by a soil *Streptomyces* sp. promotes plant defense
648 responses against fungal infection. *Mol. Plant-Microbe Interact.* **33**, 223-234 (2020).
649 54. Li, X., Tian, Y., Peng, H., He, B. & Gao, K. Isolation, screening and identification of an antagonistic
650 actinomycetes to control *Fusarium* wilt of *Momordica charantia*. *Ying Yong Sheng Tai Xue Bao* **31**,
651 3869-3879 (2020).
652 55. Yun, T., et al. Anti-Foc RT4 activity of a newly isolated *Streptomyces* sp. 5-10 from a medicinal

653 plant (*Curculigo capitulate*). *Front. Microbiol.* **11**, 610698 (2021).
654 56. Chung, Y., et al. Comparative genomics reveals a remarkable biosynthetic potential of the
655 *Streptomyces* phylogenetic lineage associated with rugose-ornamented spores. *Msystems* **6**, e00489-21
656 (2021).
657 57. Jiang, M., et al. GdmRIII, a TetR family transcriptional regulator, controls geldanamycin and
658 elaiophylin biosynthesis in *Streptomyces autolyticus* CGMCC0516. *Sci. Rep.* **7**, 4803 (2017).
659 58. He, W., et al. Crossregulation of rapamycin and elaiophylin biosynthesis by RapH in *Streptomyces*
660 *rapamycinicus*. *Appl. Microbiol. Biotechnol.* **106**, 2147-2159 (2022).
661 59. Raaijmakers, J. & Kiers, E. Rewilding plant microbiomes. *Science* **378**, 599-600 (2022).
662 60. Tsugawa, H., et al. MS-DIAL: data-independent MS/MS deconvolution for comprehensive
663 metabolome analysis. *Nat. Methods* **12**, 523-526 (2015).
664 61. Madeira, F., et al. Search and sequence analysis tools services from EMBL-EBI in 2022. *Nucleic*
665 *Acids Res.* **50**, W276-W279 (2022).
666 62. Letunic, I. & Bork, P. Interactive Tree Of Life (iTOL) v5: an online tool for phylogenetic tree
667 display and annotation. *Nucleic Acids Res.* **49**, W293-W296 (2021).

668 **Acknowledgements**

669 We acknowledge Dr. Yaojun Tong for the discussions on CRISPR-BEST. We thank the support from
670 Dr. Charlotte Held Gotfredsen (DTU NMR Centre), and Dr. Aaron John Christian Andersen (DTU
671 Metabolomics Core). We acknowledge financial support from Carlsberg Infrastructure (CF20-0177),
672 Novo Nordisk Foundation Proof of Concept (NNF20OC0062267), DTU Enable Program,
673 InnoExplorer Grant, Innovation Fund Denmark, and Danish National Research Foundation (DNRF137)
674 for support towards the Centre for Microbial Secondary Metabolites (CeMiSt). Z.Y. acknowledges
675 funding from the China Scholarship Council (202004910340). T.W. acknowledges funding from the
676 Novo Nordisk Foundation (NNF20CC0035580).

677 **Author contributions**

678 Z.Y. and T.W. designed and carried out genetic experiments and bioinformatic analyses. E.S. isolated
679 the metabolites and characterised the structures; L.D. did structure elucidation, compounds crystalision,
680 and preliminary plant assays; Z.Y., Y.Q., N.C.K. and E.A. performed the plant and qRT-PCR assays;
681 G. P. and M. A. carried out large scale fermentation and downstream processing; P.H. carried out X-
682 ray crystallography and data analysis. All the authors discussed the results and commented on the
683 manuscript.

684 **Competing interests**

The authors declare no competing interests.

Correspondence and requests for materials should be addressed to Ling Ding.

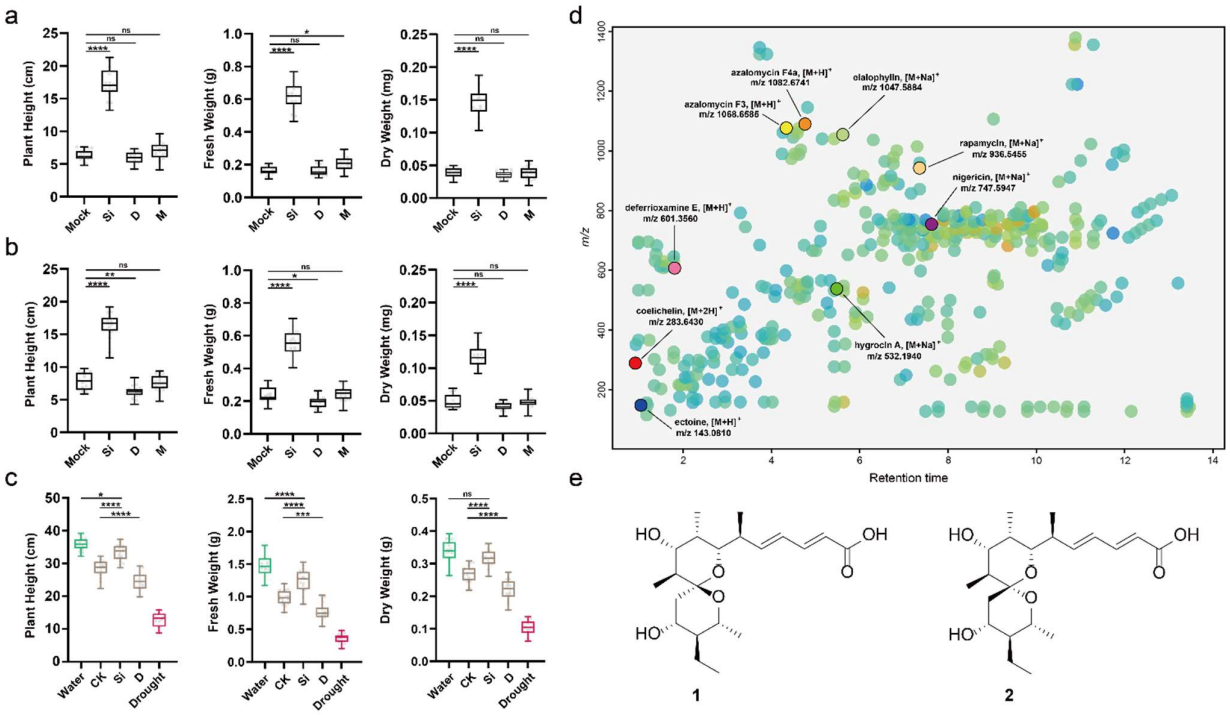

Fig. 1. The effect of *S. iranensis* on barley seedlings under the abiotic stress and the bioactive components produced by *S. iranensis*. ***a***, the box plots (middle bar=median, box limit=upper and lower quartile, extremes=min and max values) depict the plant height, fresh weight and dry weight of barley seedlings growing under osmotic stress mediated by 20% (w/v) PEG-6000 (*n*=18). Abbreviation: ***Mock***, control; ***Si***, treatment of *S. iranensis* culture broth; ***D***, treatment of *S. iranensis*/Δ*ptaA* culture broth; ***M***, treatment of blank medium (ISP2); Statistical significance was assessed by one-way ANOVA with post hoc Dunnett's multiple comparisons test. ***b***, the box plots depict the plant height, fresh weight and dry weight of barley seedlings growing under salinity stress mediated by 100 mM NaCl (*n*=18). Abbreviation: ***Mock***, control; ***Si***, treatment of *S. iranensis* culture broth; ***D***, treatment of *S. iranensis*/Δ*ptaA* culture broth; ***M***, treatment of blank medium (ISP2). Statistical significance was assessed by one-way ANOVA with post hoc Dunnett's multiple comparisons test. ***c***, the box plots depict the plant height, fresh weight and dry weight of barley seedlings growing under drought stress (*n*=18). Different colours of box plots indicate different growing conditions: green, 21 days water; brown, 7 days treatment after 7 days water followed by 7 days drought; red, 7 days water followed by 14 days drought. Statistical significance was assessed by one-way ANOVA with Tukey test. Abbreviation: ***Water***, well water for 21 days; ***CK***, 7 days treatment of water after 7 days water + 7 days drought; ***Si***, 7 days treatment of *S. iranensis* culture broth after 7 days water + 7 days drought; ***D***, 7 days treatment of *S. iranensis*/Δ*ptaA* culture broth after 7 days water + 7 days drought; ***M***, treatment of blank medium (ISP2); ***Drought***, 14 days drought after 7 days water. Statistical significance was assessed by one-way ANOVA with Tukey test. ***d***, the metabolite profile of the native *S. iranensis* growing in liquid ISP2 medium, the known secondary metabolites were identified by HR-LC-MS/MS and highlighted; ***e***, the bioactive components pteridic acid H (**1**) and pteridic acid F (**2**) isolated from *S. iranensis*.

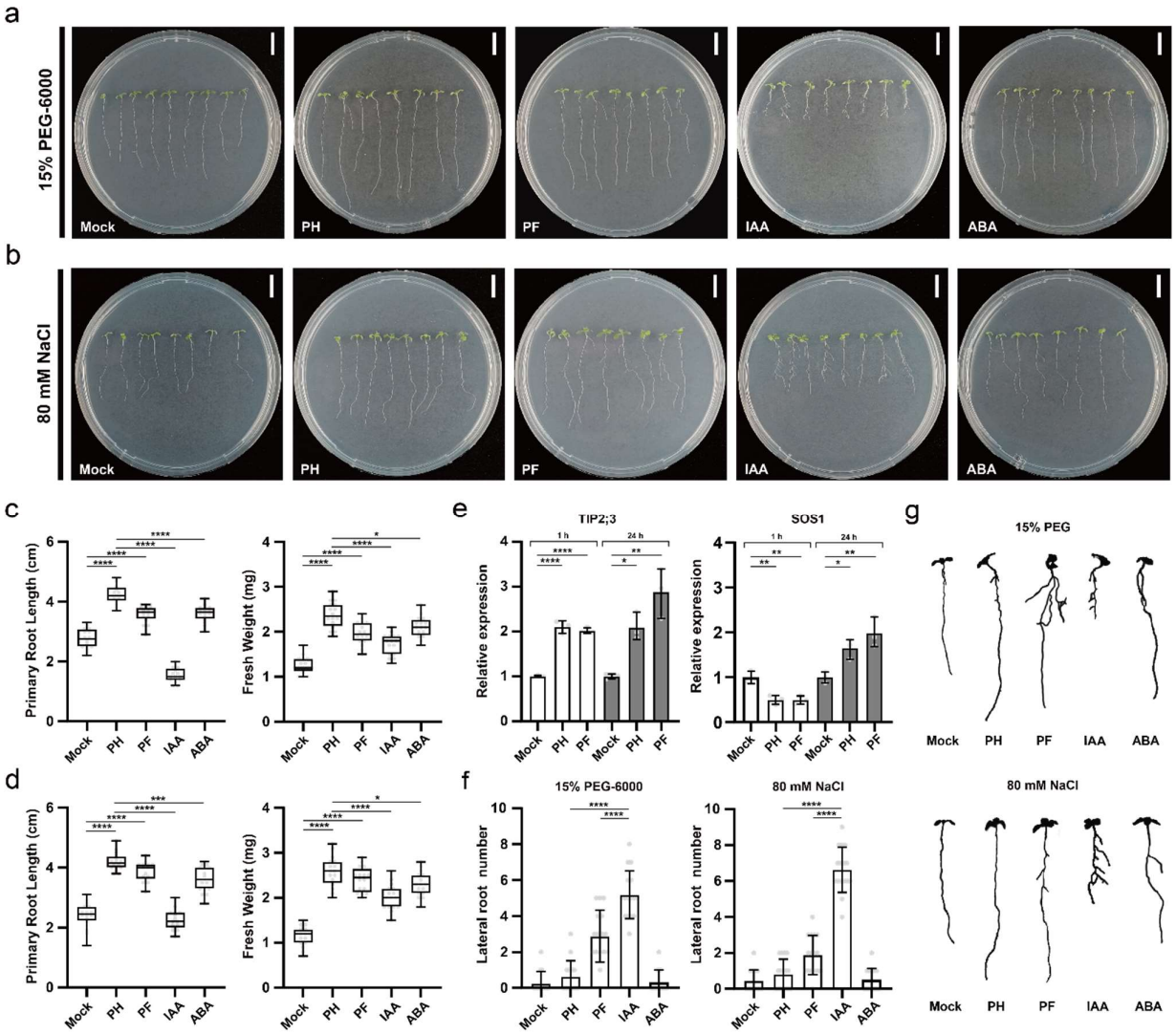

Fig. 2. The effect of pteridic acids H and F on *Arabidopsis* seedlings under abiotic stress. ***a***, phenotype of *Arabidopsis* seedlings growing under drought stress mediated by 15% (w/v) PEG-6000 using other treatments (bars=1 cm); ***b***, phenotype of *Arabidopsis* seedlings growing under salinity stress mediated by 80 mM NaCl using other treatments (bars=1 cm); ***c***, the box plots (middle bar=median, box limit=upper and lower quartile, extremes=min and max values) depict the primary root length and fresh weight of *Arabidopsis* seedlings growing on non-stress condition (n=16). Statistical significance was assessed by one-way ANOVA with Tukey test; ***d***, the box plots depict the primary root length and fresh weight of *Arabidopsis* seedlings growing on drought stress condition (n=16). Statistical significance was assessed by one-way ANOVA with Tukey test; ***e***, the relative expression level of TIP2;3 and SOS1 in *Arabidopsis* seedlings under salinity stress were measured after 1 hour and 24 hours of different treatments. Each treatment contains three biological replicates. Statistical significance was assessed by one-way ANOVA with post hoc Dunnett's multiple comparisons test; ***f***, the lateral root number of *Arabidopsis* seedlings growing in different conditions (n=16). Statistical significance was assessed by one-way ANOVA with post hoc Dunnett's multiple comparisons test. ***g***, the phenotype differences of lateral root growth of *Arabidopsis* seedlings growing in other conditions. Abbreviations: ***Mock***, control; ***PH***, treatment of 0.5 ng mL^{-1} pteridic acid H; ***PF***, treatment of 0.5 ng mL^{-1} pteridic acid F; **IAA**, treatment of 1.3 nM indole-3-acetic acid; ***ABA***, treatment of 1.3 nM abscisic acid.

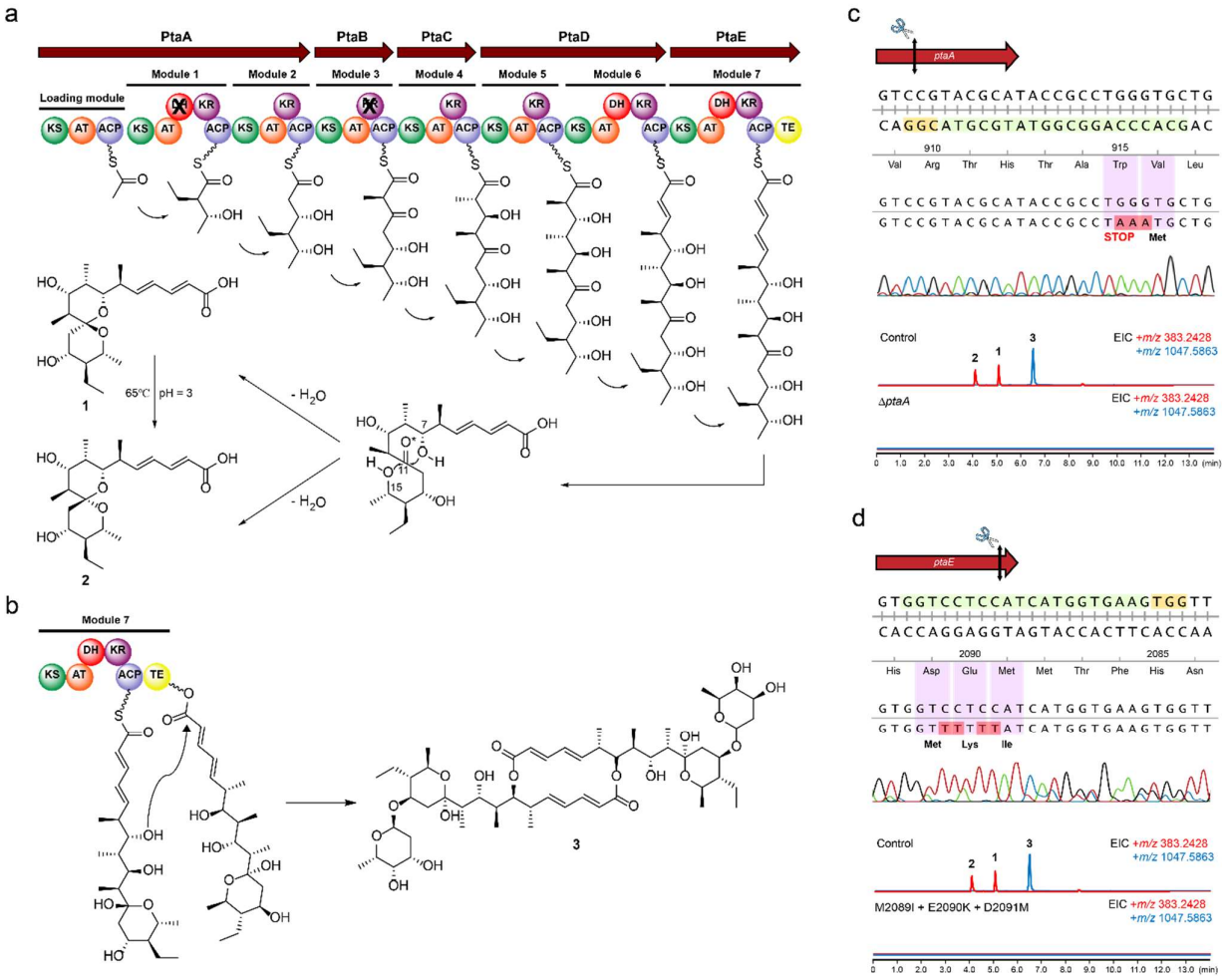

Fig. 3. Biosynthesis mechanism of pteridic acids and CRISPR base editing application in *S. iranensis*. ***a***, the proposed biosynthetic pathway of pteridic acids H (**1**) and F (**2**); ***b***, the proposed biosynthesis mechanism of elaiophylin (**3**), and its macrodiolide formation is catalysed by thioesterase (TE) domain. ***c***, Sanger sequencing and LC-MS/MS output of CRISPR base editing application of STOP codon introduction targeting the *ptaA* of *S. iranensis*. The 20-nt protospacer sequence is highlighted in light green, whereas the 3-nt PAM sequence is shown in yellow. The codons and corresponding amino acids are indicated, and the black double-headed arrow represents the position of the editing window; ***c***, Extracted Ion Chromatography (EIC) for **1** and **2** (*m/z* 383.2428 $[M+H]^+$) and **3** (*m/z* 1047.5863 $[M+Na]^+$) in the wild type *S. iranensis* (Control) and the mutant *S. iranensis*/Δ*ptaA*; ***d***, Sanger sequencing and LC-MS/MS output of CRISPR base editing application of site-directed mutagenesis targeting the TE domain of *pta* BGC. EIC for **1** an **2** (*m/z* 383.2428 $[M+H]^+$) and **3** (*m/z* 1047.5863 $[M+Na]^+$) in the wild type *S. iranensis* (Control) and the mutant *S. iranensis/*M2089I + E2090K + D2091M.

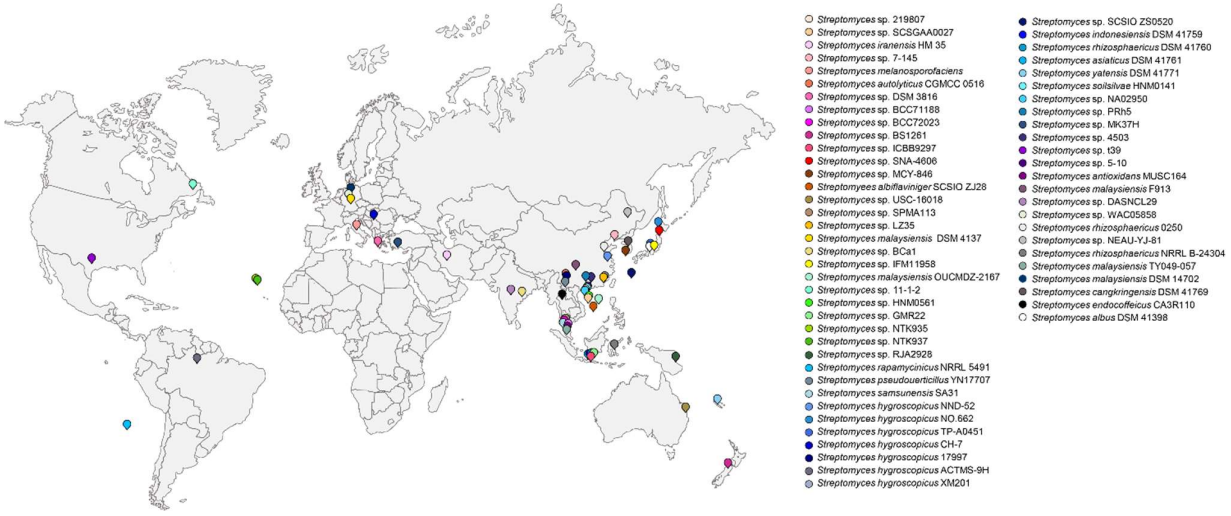

Fig. 4. Geographical distribution of *pta*-containing *Streptomyces* strains possessing *pta* BGC. A total of 62 *Streptomyces* strains were displayed on the map and distinguished by different colours. For detailed strain information, see Supplementary Tab. 4.

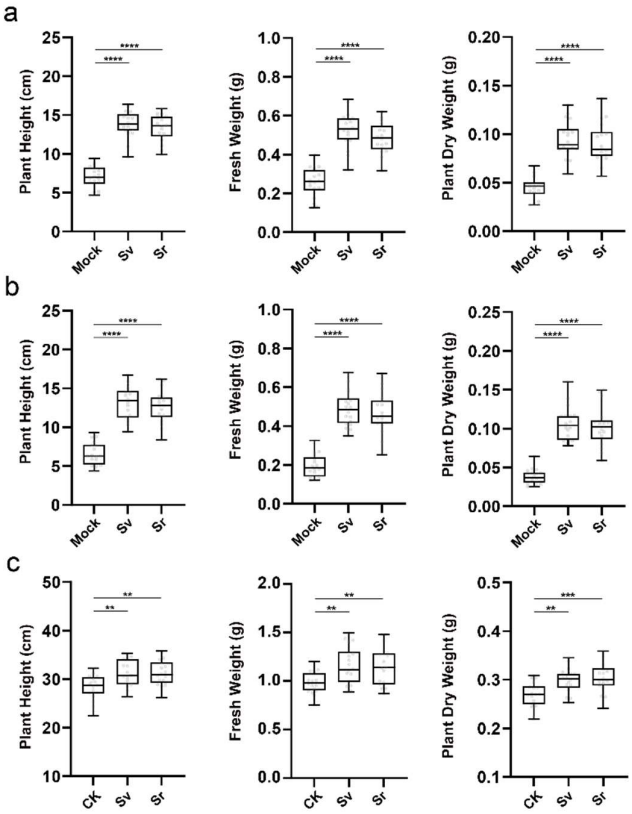

Fig. 5. Abiotic stresses alleviation led by *S. violaceusniger* Tu 4113 and *S. rapamycinicu*s NRRL 5491. ***a***, the box plots (middle bar=median, box limit=upper and lower quartile, extremes=min and max values) shows different growth of barley seedlings in osmotic stress mediated by 20% (w/v) PEG-6000 (n=16). Abbreviation: ***Mock***, control; ***Sv***, treatment of *S. violaceusniger* Tu 4113 culture broth; ***Sr***, treatment of *S. rapamycinicus* NRRL 5491 culture broth; ***b***, different growth of barley seedlings in salinity stress mediated by 100 mM NaCl (n=16). Abbreviation: ***Mock***, control; ***Sv***, treatment of *S. violaceusniger* Tu 4113 culture broth; ***Sr***, treatment of *S. rapamycinicus* NRRL 5491 culture broth; ***c***, different growth of barley seedlings in drought stress (n=16). Abbreviation: ***CK***, 7 days treatment of water after 7 days water + 7 days drought; ***Sv***, 7 days treatment of *S. violaceusniger* Tu 4113 culture broth after 7 days water + 7 days drought; ***Sr***, 7 days treatment of *S. rapamycinicus* NRRL 5491 culture broth after 7 days water + 7 days drought. Statistical significance was assessed by one-way ANOVA with post hoc Dunnett's multiple comparisons test.

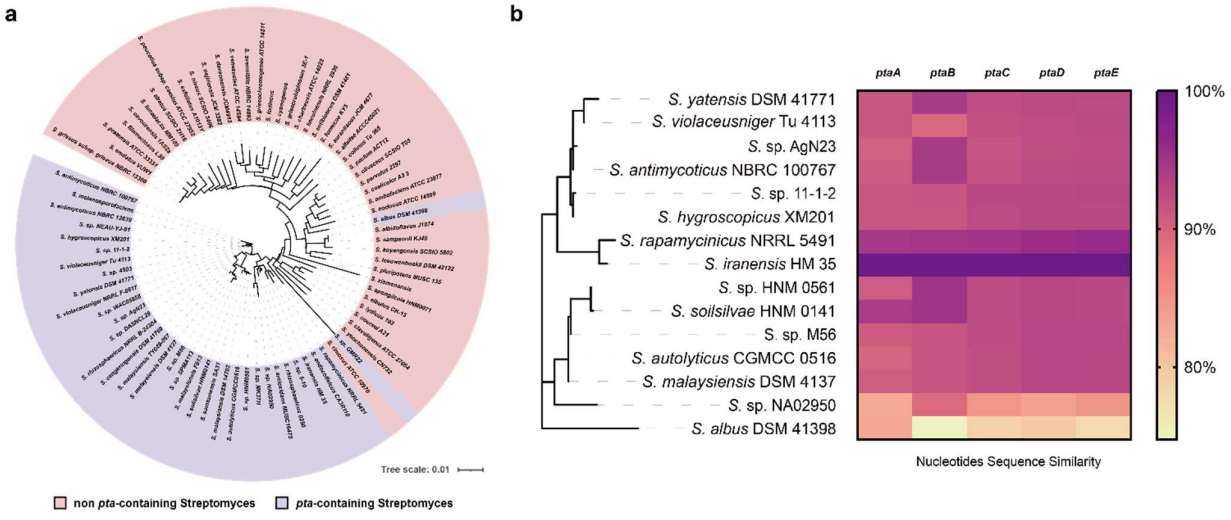

754

755 **Fig. 6**. The phylogenetic and secondary metabolites BGCs analysis of *pta*-containing *Streptomyces* strains. ***a***, the
756 phylogenetic tree of 16S rRNA nucleotides sequences of *pta*-containing *Streptomyces* and other *Streptomyces* strains;
757 ***b***, the heatmap depicts similarity differences of core biosynthetic genes of *pta* BGC between *S. iranensis* and other
758 14 *pta*-containing *Streptomyces* strains.
759